Topic number: 6

Particle simulation methods for studies of low-pressure plasma sources

Zoltán Donkó

Research Institute for Solid State Physics and Optics, Hungarian Academy of Sciences
H-1121 Budapest, Konkoly-Thege Miklós str. 29-33, Hungary
donko@mail.kfki.hu

This paper intends to illustrate the application of particle simulation methods for the description of low-pressure discharges: Townsend discharges, cathode fall dominated DC glows and capacitively coupled RF discharges. The presence of boundaries (e.g. electrodes), as well as the spatially and/or temporally varying electric field in these sources induce a non-hydrodynamic motion of some types of charged species, in particular electrons [1]. Particle based methods provide, even under non-hydrodynamic conditions, a correct way for the mathematical description of the particle transport and for the determination of the distribution functions, which are crucial quantities in discharge modeling.

Monte Carlo (MC) simulation is a widely used method to describe the motion of charged particles in a background gas [2]. Between collisions the electrons fly along trajectories derived from the integration of the equation of motion over Δt time steps. The occurrence of collisions is checked regularly for each of the particles after the Δt intervals: the collision probability for a given particle is $P = 1 - \exp[-n\sigma_{\rm tot}(\upsilon)\upsilon\Delta t]$, where n is the gas density, υ is the velocity, $\sigma_{\rm tot}$ is the total collision cross section. In studies of electron transport the target gas atoms are usually assumed to be at rest. Their thermal velocity must be taken into account only at very low fields [3]. Whenever a collision occurs, its type is chosen randomly, according to the relative magnitudes of the cross sections of different collision processes. The computational efficiency can be significantly increased by using the "null-collision" method [4], which introduces a fictitious type of collision in a way that the total collision frequency becomes constant regardless of the particle velocity. This way a time of free flight for a particle $\tau = -\ln(1-R_{01})/\nu^*$ can be assigned. R_{01} is a random number uniformly distributed over the [0,1) interval and $\nu^* = \max\{n\sigma_{\rm tot}(\upsilon)\upsilon\}$ is the maximum of the collision frequency. After this free flight a real collision occurs with a probability $P_{\rm real} = \nu_{\rm real}/\nu^*$, where $\nu_{\rm real} = n\sigma_{\rm tot}(\upsilon_{\rm coll})\upsilon_{\rm coll}$ ($\upsilon_{\rm coll}$ is the velocity right before the collision), otherwise the particle proceeds (without any change of its velocity vector) along its trajectory for a next free flight.

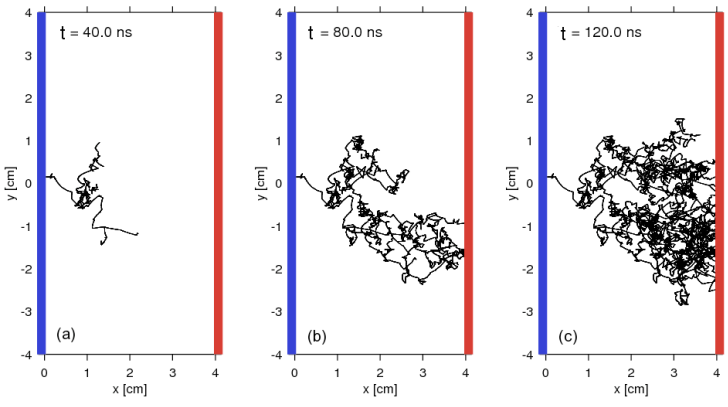

Fig. 1: Snapshots of the Monte Carlo simulation of the development of an electron avalanche in a Townsend discharge in argon, at p = 41.4 Pa and E/N = 500 Td. The cathode is situated at x = 0, while the anode is at x = 4 cm.

Figure 1 illustrates the "visual" output of a MC simulation of the development of an electron

avalanche in argon gas, between two plane, parallel and infinite electrodes, at a reduced electric field of 500 Td. It is noted that although this setting represents the simplest possible electrode configuration, even here, the presence of boundaries induces a non-equilibrium behavior and limits the validity of a hydrodynamic approach. In the case studied (i) we find an equilibration region near the cathode [5] and (ii) we expect a distortion of the distribution function near the absorbing anode (very few electrons move towards the cathode near the anode).

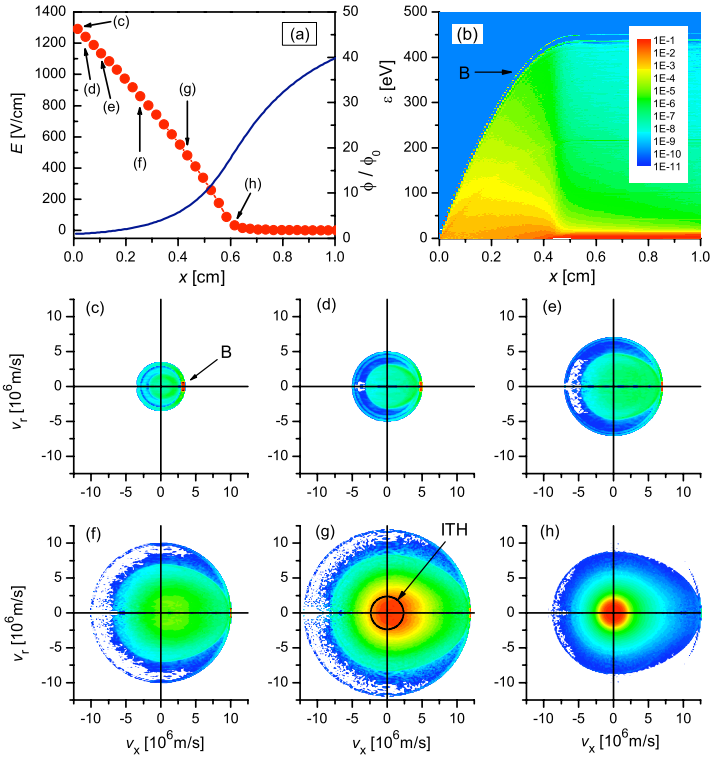

Fig. 2: Characteristics of the cathode fall region of a DC discharge in argon gas at 40 Pa and cathode fall voltage of 441 V. (a) Electric field distribution (circles, left scale) and the flux of electrons normalized to the flux at the cathode (line, right scale). (b) Color map representation of the spatial variation of the electron distribution function. (c)–(h) VDF-s of electrons at different spatial positions, between the cathode and the sheath – glow boundary, defined in panel (a); the color scale of the VDF-s is logarithmic and spans four orders of magnitude. "B" in (b) and (c) indicates a beam of electrons propagating away from the cathode. The circle labeled as "ITH" in (g) shows the velocity corresponding to the ionization threshold.

Monte Carlo simulation of the particles (mostly of "fast" electrons) have also been routinely applied in the models of glow discharges, often combined with the fluid description of "slow" plasma species. Models that combine these approaches have been termed as "hybrid models" [6]. The importance of the kinetic treatment of fast electrons in the DC cathode sheath lies in the possibility of obtaining an accurate ionization source function, which was proved to be critical for a precise description of this region [7]. Kinetic treatment of fast electrons is also necessary in order to reproduce the experimentally observed distribution of light emission of the discharge [8]. In Figure 2 results for the classical example of the electron transport through a DC cathode sheath are presented (similarly to the pioneering studies of [9]), focusing on the spatial evolution of the electron velocity distribution function (VDF).

Another particle-based approach, most popular for the description of radiofrequency discharges, is the Particle-in-Cell (PIC) method [10]. The PIC approach uses superparticles, which represent many (typically 10^5 – 10^6) real particles. At each time step the charge of these particles

Topic number: 6

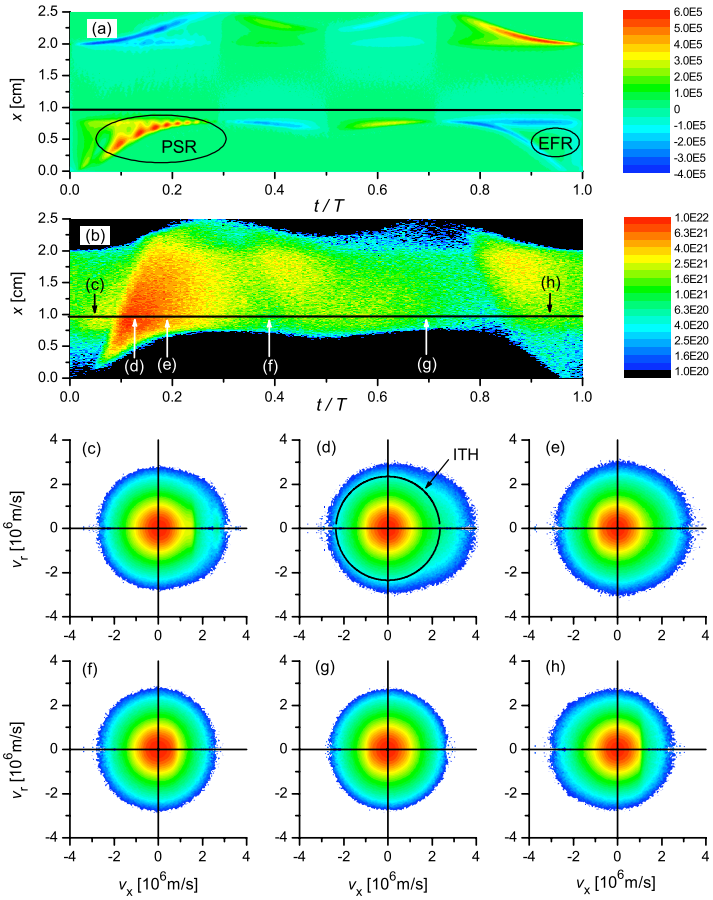

Fig. 3: Spatio-temporal distributions of (a) the electron heating rate and (b) ionization rate in a dual-frequency RF discharge driven by 500 V voltage amplitude at both 13.56 MHz and 27.12 MHz frequencies (at $\theta = 0°$), at $p = 5$ Pa, $L = 2.5$ cm. The coordinate x is measured from the powered electrode, T is the period of the 13.56 MHz signal. The heating rate is given in units of W/m^3, the ionization rate is given in units of 1/(m^{3}s). "PSR" denotes a region where Plasma Series Resonance oscillations modulate the heating rate and "EFR" denotes a region of Electric Field Reversal [11] in panel (a). (c)-(h): electron VDF-s at different times indicated in (b), at a spatial coordinate $x = 0.96$ cm. Note the asymmetry, which is most pronounced in (d) and (h) due to the expansion of the powered and grounded sheaths, respectively. The black circle (labeled "ITH") in (d) corresponds to the velocity at ionization threshold. The color scale in (c)-(h) is logarithmic and covers four orders of magnitude.

is assigned to a grid, and the potential distribution is calculated from the charge distribution, taking into account the potentials applied to the electrodes, as boundary conditions. The forces acting on the particles are obtained by differentiation of the potential and interpolation of the resulting electric field to the positions of the particles. The new positions and velocities are obtained from the solution of the equation of motion. Collisions between the traced charged particles and the atoms of the background gas can be incorporated into the PIC scheme using a Monte Carlo approach (PIC/MCC). For electrons elastic scattering, excitation and ionization are commonly considered. Attachment processes (negative ion formation), recombination processes, as well as Coulomb collisions between the charged particles may also be included in the simulations. It is noted that the kinetic properties of the PIC method were found to be affected by inclusion of the collisions [12]. Nonetheless, PIC/MCC simulations provide a detailed insight into the physics of RF plasma sources by delivering spatio-temporal distributions of quantities of interest: particle distribution

functions, the ionization and excitation rates, the electron heating rate, as well as the fluxes and densities of different species.

As an example here we take a RF discharge, which operates under the conditions of the Electrical Asymmetry Effect (EAE). The EAE [13] in geometrically symmetric reactors can be realized by driving the discharge with two frequencies: a base frequency f and its second harmonic $2f$. The locked, but adjustable phase angle between the two sources results in the development of a DC self bias η in the discharge, which gives a possibility for a nearly independent control of the ion flux and ion energy at the electrodes. Figure 3 displays the results of a PIC/MCC simulation of a discharge excited by a voltage $V(t) = V_0[\cos(\omega t + \theta) + \cos(2\omega t)]$, at $p = 5$ Pa, $L = 2.5$ cm, V_0 = 500 V. For the present case $\theta = 0^\circ$ is chosen, which results in a bias of η = -370 V.

Figures 3 (a) and (b) show two spatio-temporal distributions, related to acquiring (heating rate, (a)) and depositing (ionization rate, (b)) electron energy. Both exhibit strongly asymmetric patterns. The highest ionization rate is found to be induced by the electrons accelerated towards the bulk plasma by the expansion of the powered sheath. At this phase "Plasma Series Resonance" oscillations [14] are observed in the plot of the heating rate (indicated as "PSR" in panel (a)). The grounded sheath expands twice during the period of the lower frequency T = 1/13.56 MHz, but both of these expansions create less significant beams of electrons. Panels (c)-(h) of Figure 3 display the VDF-s of the electrons at certain times, at a fixed position in the discharge gap, indicated by the horizontal thick black line in panel (b). Distortion (asymmetry) of the VDF-s is seen at almost all times, the most significant asymmetry occurring in (d), at $t/T \cong 0.13$. Here a high velocity beam of electrons propagating into the positive x direction is observed. A weaker distortion in the $-x$ direction is observed in panel (h), caused by the beam of electrons originating from the sheath expansion at the grounded electrode.

The author thanks his numerous collaborators and the Hungarian Scientific Research Fund (OTKA, current grant K77653) for having supported his work for 20 years.

Reference

[1] Robson R E, White R D, Petrović Z Lj 2005 *Rev. Mod. Phys.* **77** 1303; Pitchford L C, Boeuf J-P, Segur P, Marode E 1990 in *Non-equilibrium Effects in Ion and Electron Transport*, ed. Gallagher J W (Plenum, New York); Tsendin L D 1995 *Plasma Sources Sci. Technol.* **4** 200; Tsendin L D 2009 *Plasma Sources Sci. Technol.* **18** 014020; Kudryavtsev A A, Morin A V, Tsendin L D 2008 *Tech. Phys.* **53** 1029

[2] Longo S 2006 *Plasma Sources Sci. Technol.* **15** S181

[3] Yousfi M, Hennad A, Alkaa A 1994 *Phys. Rev. E* **49** 3264

[4] Skullerud H R 1968 *J. Phys. D* **1** 1567

[5] Malović G, Strinić A, Živanov A, Marić D, Petrović Z Lj 2003 *Plasma Sources Sci. Technol.* **12** S1

[6] Surendra M, Graves D B, Jellum G M 1990 *Phys. Rev. A* **41** 1112; Boeuf J-P and Pitchford L C 1991 *IEEE Trans. Plasma Sci.* **19** 286; Bogaerts A, Gijbels R, Goedheer W J 1996 *Anal. Chem.* **68** 2296; Donkó Z 2001 *Phys. Rev. E* **64** 026401; Brok W J M, Wagenaars E, van Dijk J, van der Mullen J J A 2007 *IEEE Trans. Plasma Science* **35** 1325

[7] Derzsi A, Hartmann P, Korolov I, Karácsony J, Bánó G, Donkó Z 2009 *J. Phys. D* **42** 225204

[8] Rózsa K, Gallagher A, Donkó Z 1995 *Phys. Rev. E* **52** 913; Marić D, Kutasi K, Malović G, Donkó, Petrović Z Lj 2002 *Eur. Phys. J D* **21** 73

[9] Boeuf J P and Marode E 1982 *J. Phys. D* **15** 2169

[10] Birdsall C K 1991 *IEEE Trans. Plasma Sci.* **19** 65

[11] Schulze J, Donkó Z, Heil B G, Luggenhölscher D, Mussenbrock T, Brinkmann R P, Czarnetzki U 2008 *J. Phys. D* **41** 105213

[12] Turner M M 2006 *Phys. Plasmas* **13** 033506

[13] Heil B G, Czarnetzki U, Brinkmann R P, Mussenbrock T 2008 *J. Phys. D* **41** 165202

[14] Donkó Z, Schulze J, Czarnetzki U, Luggenhölscher D 2009 *Appl. Phys. Lett.* **94** 131501